AIAA JOURNAL
Vol. 30, No. 9, September 1992

Damage Detection in Elastic Structures Using Vibratory Residual Forces and Weighted Sensitivity

J. M. Ricles* and J. B. Kosmatka†
University of California, San Diego, La Jolla, California 92093

A methodology is presented for detecting structural damage in elastic structures by nondestructive means. Measured modal test data along with a correlated analytical structural model are used to locate potentially damaged regions using residual modal force vectors and to conduct a weighted sensitivity analysis to assess the extent of mass and/or stiffness variations, where damage is characterized as a stiffness reduction. The current approach is unique among other approaches in that it accounts for 1) variations in system mass, system stiffness, and mass center locations, 2) perturbations of both the natural frequencies and modal vectors, and 3) statistical confidence factors for the structural parameters and potential experimental instrumentation error. Moreover, this procedure can be used with either full or reduced models. A wide variety of numerical examples are presented that show that the current method provides a precise indication of both the location and the extent of structural damage.

Introduction

FLEXIBLE space structures, launch vehicles, and satellites are susceptible to structural damage over their operating lives from impact, operating loads, and fatigue. Undetected and uncorrected damage can lead to structural deterioration of their members and consequently jeopardize the flight safety of the structure. Thus, numerous damage inspection methods and monitoring procedures have been developed. Examples include x-ray, ultrasonic testing, magnetic resonance, coin tap, dye penetration, and visual inspection. These methods can be time consuming and are local assessments, often requiring the exposure of structural elements to the inspector and equipment for detecting damage. As a monitoring system for detecting damage of spacecraft in orbit (i.e., Space Station Freedom), none of these methods are appropriate. An alternative approach, which formed the basis for our current study, is to recognize the fact that modal vibration test data (structural natural frequencies and mode shapes) characterize the state of the structure.[1] Therefore, postflight and in-flight (e.g., monitoring) data can be used to distinguish whether changes (damage) have occurred to the structure by comparing these data with a set of baseline data. Modal testing as a means of inspection has several advantages. Direct exposure of structural elements is not required, and at the same time more of the complete structure can be inspected in one modal test by having appropriately placed sensors. The consequences of this are a reduction in schedule and cost.

The use of vibration test data to locate structural damage has been attempted to evaluate the integrity of offshore oil and gas platforms,[2,3] composite laminates,[4] continuum structures,[5-8] and recently large space structures.[9-11] The early analytical and experimental approaches[2,3] had limited success as a result of inadequate instrumentation and addressing only frequency shifts associated with stiffness changes, while ignoring changes in the modal vectors. The continuum-based methods[5-8] provide valuable insight into the magnitude of frequency shifts, but their usefulness is severely limited to simple structures (bars, beams, plates) with unrealistic boundary conditions. Two of the methods which are applicable to large space structures[9,10] are for the most part applications of existing system identification techniques.[12-14] Smith and Hendricks[9] discovered through a series of numerical examples that two well-known system identification techniques[12,13] were unable to detect damage to a three-dimensional space truss model. Chen and Garba[10] developed a three-step damage detection procedure, based on Ref. 14, that initially uses residual force vectors to locate potential damage areas; next a least-squares approach is used to determine scalars for the appropriate element stiffness matrices; and finally damage is located in the structural members where the calculated element scalars are less than unity. All of the aforementioned approaches ensure that the original structural connectivity is retained but the approaches are severely limited with the assumption that the system mass is constant and changes in vibration characteristics are associated with only stiffness variations. This is unrealistic for a large flexible space structure, where frequency shifts can be expected to occur as a result of mass variations associated with the movement of antennas, astronauts, and solar arrays; docking of visiting spacecraft; or changing levels in fluid containers. Furthermore, these approaches do not account for the mode shape variations, uncertainty in the structural parameters, and instrumentation accuracy. Recently Stubbs[11] studied damage detection in large space structures by treating the three-dimensional space truss as an equivalent Euler-Bernoulli beam. This simplistic approach accounted for changes to both mass and stiffness, but ignored the sensitivity of the mode shapes to damage.

The purpose of the current study is to develop a new methodology for nondestructively detecting damage in flexible space structures. This methodology uses measured modal data along with a correlated analytical structural model first to locate potentially damaged regions using residual modal force vectors (based on Refs. 10 and 14) and then to conduct a weighted sensitivity analysis (based on Ref. 15) to assess the extent of mass and/or stiffness variations, where damage is characterized as a stiffness reduction. The current approach is unique among all existing approaches in that it accounts for 1) variations in system mass, system stiffness, and mass center locations; 2) perturbations of both the natural frequencies and modal vectors; and 3) statistical confidence factors for the structural parameters and potential experimental instrumentation error. Moreover, this procedure can be used with either full or reduced models. Numerical results are presented to validate and assess the current approach using analytically derived modal test data for a number of different cases, repre-

Received Sept. 17, 1991; revision received Jan. 23, 1992; accepted for publication Feb. 3, 1992.

*Assistant Professor, Department of Applied Mechanics and Engineering Science.

†Assistant Professor, Department of Applied Mechanics and Engineering Science. Member AIAA.

senting damage scenarios involving two different truss-type structures. Damage location and extent are determined for all cases.

Theoretical Basis

The methodology for the current nondestructive damage detection procedure is presented in Fig. 1, where the algorithm consists of three main steps: 1) modal testing, 2) location of potential damage regions, and 3) assessment of damage. In the modal testing step, an experimental modal survey is performed on the initial (undamaged) structure to measure the system vibration properties Λ_0, which include the natural frequencies ω_0 and mode shapes Φ_0. These experimental data, along with an existing system identification technique,[12-15] are used to develop a correlated "baseline" (undamaged) analytical model, where the corresponding analytical vibration properties are given as Λ_a, with mode shapes and natural frequencies defined as Φ_a and ω_a, respectively. This analytical model is used as a basis for subsequent comparison in the remaining two algorithm steps. A postflight (or in-flight for real-time monitoring) experimental modal survey is performed to measure the vibration properties Λ_d, which includes natural frequencies ω_d and mode shapes Φ_d. The subscript d is used to symbolize the structure configuration that includes the (potential) damage.

The selection of which experimental natural frequencies and mode shapes in Λ_0 and Λ_d are to be used in the damage detection algorithm depends on how well the baseline analytical model Λ_a correlates to the initial (undamaged) structure Λ_0. If the vibration properties of Λ_a exactly correlate to Λ_0, then one is free to select any combination of modes, where this modal set should have an adequate level of modal strain energy in all structural components. If the vibration properties of Λ_a are not exactly correlated to Λ_0, then one should select only those modes of Λ_d where discrepancies between Λ_0 and Λ_a are smaller than those of Λ_0 and Λ_d. Otherwise these initial errors will incorrectly dominate the estimated damage. The mode selection process should be based on the following criteria: a smaller frequency shift $\Delta\omega$ as well as a superior set of modal assurance criterion (MAC) values between Λ_0 and Λ_a compared with Λ_0 and Λ_d, and an adequate cross-orthogonality check (COR) between Λ_0 and Λ_a, where for the ith mode (considering Λ_0 and Λ_a)

$$\Delta\omega_i = (\omega_i)_0 - (\omega_i)_a \tag{1}$$

$$\mathrm{MAC}_i = \frac{\left[\sum_{j=1}^{N} (\phi_{ji})_0 (\phi_{ji})_a\right]^2}{\sum_{j=1}^{N} (\phi_{ji})_0^2 \sum_{j=1}^{N} (\phi_{ji})_a^2} \tag{2}$$

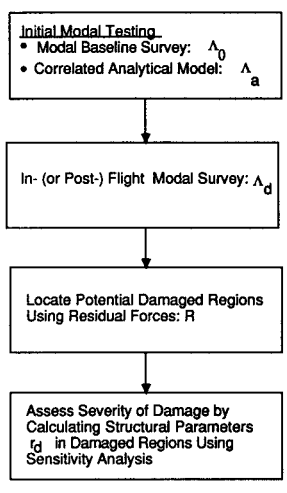

Fig. 1 Damage detection algorithm.

and for all modes

$$\mathrm{COR} = \Phi_0^T M_a \Phi_a \tag{3}$$

in which M_a is the analytical mass matrix, and j is the instrumentation point location. The assessment for $\Lambda_0 - \Lambda_d$ is performed by replacing Λ_a with Λ_d in Eqs. (1-3).

Location of Potential Damage Regions

Identifying the location of damage in the structure is based on differences in Λ_d and Λ_0 through an extended application of the residual force method (see Ref. 10 for further details). In concept, the experimental natural frequencies and mode shapes must satisfy an eigenvalue equation, where considering the ith mode of the potentially damaged (postflight) structure

$$(K_d - \lambda_{d_i} M_d)\phi_{d_i} = 0 \tag{4}$$

in which K_d and M_d are the experimental (unknown) stiffness and mass matrices associated with the damaged structure, respectively, and $\lambda_{d_i}(\omega_{d_i}^2)$ is the experimental measured eigenvalue (natural frequency squared) corresponding to the experimental measured ith mode shape ϕ_{d_i} of the damaged structure. Assuming that the stiffness and mass matrices associated with the damaged structure are defined as

$$K_d = K_a + \Delta K \tag{5a}$$

$$M_d = M_a + \Delta M \tag{5b}$$

where K_a and M_a are the baseline stiffness and mass matrices of the analytical model, respectively, and ΔK and ΔM are the unknown changes in the stiffness and mass matrices as a result of damage, respectively. Substituting Eq. (5) into Eq. (4) and rearranging, one arrives at the definition of the residual force vector for the ith mode (R_i):

$$R_i = -(\Delta K - \lambda_{d_i} \Delta M)\phi_{d_i} \tag{6a}$$

$$= (K_a - \lambda_{d_i} M_a)\phi_{d_i} \tag{6b}$$

where the right-hand side of Eq. (6b) is known and will only equal zero if (λ_{d_i}, ϕ_{d_i}) are equal to the undamaged (baseline) values (λ_{a_i}, ϕ_{a_i}). Regions within the structure that are potentially damaged correspond to the degrees of freedom (DOF) that have large magnitudes in R_i. It should be emphasized that one should calculate the residual force R_i using many different modes because if a damaged member is located near a node line, then the modal displacement is near zero and the residual force will also be near zero.

Assessment of Damage Severity

The assessment of damage severity is based on establishing a relationship between the measured vibration characteristics and the structural parameters (members mass, stiffness, section geometry) in the damaged region using a first-order Taylor series expansion:

$$\Lambda_d = \Lambda_0 + T(r_d - r_0) + \epsilon \tag{7}$$

where Λ_0 and Λ_d are arrays containing the selected, experimentally measured natural frequencies and mode shapes of the initial (undamaged) and damaged structures, respectively [with $\Lambda^T = (\omega^2, \Phi)^T$]; r_d is an array of the unknown structural parameters in the damaged region; r_0 is an array of the initial (known) structural parameters in the same damaged region; and ϵ is an array of testing errors associated with each measured parameter (i.e., mode shape amplitudes and natural frequencies). Matrix T is a sensitivity matrix that relates the

change in the structural parameters to changes in the vibration properties (natural frequencies and mode shapes):

$$T = \begin{bmatrix} \frac{\partial\omega^2}{\partial K} & \frac{\partial\omega^2}{\partial M} \\ \frac{\partial\Phi}{\partial K} & \frac{\partial\Phi}{\partial M} \end{bmatrix}_0 \begin{bmatrix} \frac{\partial K}{\partial r} \\ \frac{\partial M}{\partial r} \end{bmatrix}_0 \tag{8}$$

where the subscript 0 is associated with the initial (baseline) configuration. The four submatrices in the first matrix of T represent partial derivatives of the eigenvalues and mode shapes with respect to the coefficients of the stiffness and mass matrices, whereas the second matrix of T represents the partial derivatives of the stiffness and mass matrices with respect to the structural parameters r. The derivatives of the eigenvalues and mode shapes are determined using the experimentally measured vibration properties of the initial (undamaged) structure Λ_0 and baseline analytical mass matrix M_a, where for mode k and considering instrumentation points i and j it can be shown (from Refs. 15–17)

$$\frac{\partial\omega_k^2}{\partial K_{ij}} = \frac{\phi_{ik}\phi_{jk}}{\phi_k^T M_a \phi_k} \tag{9a}$$

$$\frac{\partial\phi_{rk}}{\partial K_{ij}} = \sum_{n=1}^{q}\left[\frac{\phi_{in}\phi_{jk}\phi_{rn}}{(\omega_k^2 - \omega_n^2)\phi_n^T M_a \phi_n}\right](1 - \delta_{nk}) \tag{9b}$$

$$\frac{\partial\omega_k^2}{\partial M_{ij}} = -\frac{\omega_k^2\phi_{ik}\phi_{jk}}{\phi_k^T M_a \phi_k} \tag{9c}$$

$$\frac{\partial\phi_{rk}}{\partial M_{ij}} = \sum_{n=1}^{q}\left[\frac{-\omega_k^2\phi_{in}\phi_{jk}\phi_{rn}(1 - \delta_{nk})}{(\omega_k^2 - \omega_n^2)\phi_n^T M_a \phi_n} - \frac{\phi_{in}\phi_{jk}\phi_{rn}\delta_{nk}}{2\phi_n^T M_a \phi_n}\right] \tag{9d}$$

in which q is the number of retained modes in Λ_0 for the assessment and n is the index to identify mode number. For structures having repeated natural frequencies, the calculated eigenvector derivatives of Eqs. (9b) and (9c) are no longer valid and one must use an approach developed by Mills-Curan.[18]

Our goal is to determine r_d in Eq. (7). This is accomplished by first treating the difference $(r_d - r_0)$ for all structural parameters as normally distributed random variables with a zero mean and a specified covariance S_{RR} to deal with the uncertainty in the damage assessment. Treating the test measurement error also as a random variable with a zero mean and specified covariance $S_{\epsilon\epsilon}$ leads to the solution for r_d from Ref. 15 as

$$r_d = r_0 + S_{RR}^* T^T (T S_{RR}^* T^T + S_{\epsilon\epsilon})^{-1}(\Lambda_d - \Lambda_0) \tag{10a}$$

where

$$S_{RR}^* = S_{RR} - S_{RR} T^T (T S_{RR} T^T + S_{\epsilon\epsilon})^{-1} T S_{RR} \tag{10b}$$

Values for the diagonal terms (e.g., variances) in S_{RR} are assigned in conjunction with the results of the residual force analysis and all off-diagonal terms are set equal to zero. Only those members suspected of damage are given nonzero variances, and therefore these are the only members that are emphasized in the damage severity assessment. In the current study, all suspected members with damage were given equal variances. It should be noted that uncertainties associated with the structural parameters of the analytical model can also be considered by assigning nonzero variances. The matrix $S_{\epsilon\epsilon}$ is usually treated as diagonal since the measurement errors are statistically independent. The magnitude of the diagonal values of $S_{\epsilon\epsilon}$ can sometimes be difficult to estimate, and it is important to be conservative.

If the relationship between the stiffness and mass components and the structural system is linear, the current method [Eq. (10)] will converge in one step. However, the partial derivatives of the eigenvalues with respect to the stiffness and mass coefficients are nonlinear if enough damage has occurred to cause a large frequency shift, as illustrated in Fig. 2a. To obtain a more accurate assessment of the severity of damage, it is necessary either to continuously monitor the system (in-flight damage monitoring) or to use the correlated analytical model to update the damage assessment to converge to Λ_d, as illustrated in Fig. 2b, where the subscripts 0, 1, and 2 refer to the linearization points during updating. Each update involves evaluating $\Delta r_i = r_d - r_i$, which represents the change in the structural parameters where r_d is from Eq. (10) considering the current structural state of $r_0 = r_i$, $T = T_i$, and $\Lambda_0 = \Lambda_i$. Here r_i is the current value for the structural parameters, which reflects the accumulated changes from the previous updates and T_i is the sensitivity matrix based on the vibration characteristics of the updated baseline analytical model (or in the case of an on-line monitoring system the measured characteristics at that time point). Convergence is achieved when Δr_i during an update becomes less than the tolerance for convergence, with the predicted extent of damage equal to the sum of Δr_i for all of the update cycles, as indicated in Fig. 2b.

In the damage detection algorithm, the full analytical model is updated, which generally has more DOF than instrumented DOF of the modal test structure. One can either use Guyan reduction to reduce the analytical model's DOF to the instrumentation points or use the full analytical model directly, where the unknown information pertaining to the noninstrumented DOF is excluded in the evaluation of T. If the first procedure is pursued, then the derivatives of the stiffness and mass coefficients with respect to the structural parameters are given as

$$\frac{\partial K_{a,ij}}{\partial r} = \frac{\partial}{\partial r}(\Psi^T K_a^* \Psi) = \frac{\partial\Psi^T}{\partial r} K_a^* \Psi + \Psi^T \frac{\partial K_{a,ij}^*}{\partial r}\Psi + \Psi^T K_a^* \frac{\partial\Psi}{\partial r} \tag{11a}$$

$$\frac{\partial M_{a,ij}}{\partial r} = \frac{\partial}{\partial r}(\Psi^T M_a^* \Psi) = \frac{\partial\Psi^T}{\partial r} M_a^* \Psi + \Psi^T \frac{\partial M_{a,ij}^*}{\partial r}\Psi + \Psi^T M_a^* \frac{\partial\Psi}{\partial r} \tag{11b}$$

where K_a and M_a are the (reduced) analytical stiffness and mass matrices, respectively, that have DOF at instrumentation points only and are defined as

$$K_a = \Psi^T K_a^* \Psi \tag{11c}$$

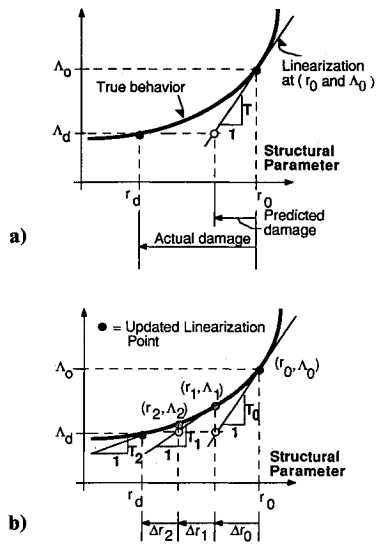

Fig. 2 Structural parameters and vibration properties: a) linearization of their nonlinear relationship, and b) updating to obtain convergence.

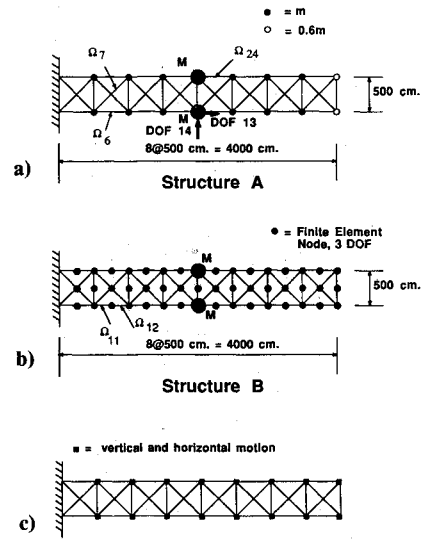

Fig. 3 Modal test: a) structure A, b) structure B, and c) instrumentation points.

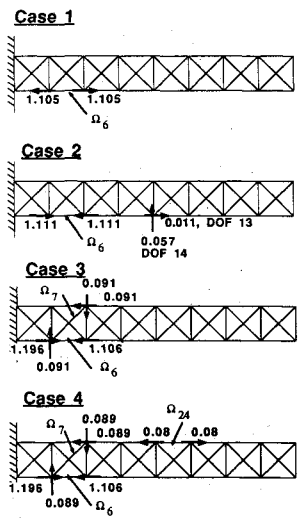

Fig. 4 Mode 1 residual forces for structure A.

$$M_a = \Psi^T M_a^* \Psi \tag{11d}$$

where K_a^* and M_a^* are the full analytical stiffness and mass matrices, and the Guyan transformation matrix Ψ is a function of the structural parameters r.

Validation and Assessment

The verification and assessment of the current damage detection methodology involves an "analytically derived modal test structure." The assessment involves imposing damage to the modal test structure and "forgetting" the location and magnitude of the imposed damage. An attempt was then made to detect the damage, using Λ_0 based on the undamaged analytical modal test model and Λ_d based on the damaged analytical modal test model.

Two structures were considered in this study. Structure A (Fig. 3a) consists of a 40-member cantilevered truss-type structure modeled using uniform bar elements [$EA = 6.784 \times 10^7$ N (1.525×10^7 lb)]. The finite element model has a total of 32 in-plane translational DOF, where 14 of the nodes have lumped mass of magnitude, $m = 403.1$ kg (2.3 lb-s^2/in.); and two of the nodes have a much larger mass of magnitude, $M = 8307.8$ kg. The larger concentrated masses, which represent nearly 75% of the total structural mass, were included to simulate components (antenna, solar arrays, fluid containers) commonly found on space structures. All 32 DOF were assumed to be instrumented (see Fig. 3c), thus no (Guyan) reduction schemes were used and the analytical baseline model (K_a, M_a) was assumed to be perfectly correlated to the initial (undamaged) experimental model so that $\Lambda_0 = \Lambda_a$. Structure B (Fig. 3b) had geometry similar to structure A, except that the mass was more evenly distributed and 80 beam elements were used instead of the previous 40 bar elements; thus the resulting model had 168 DOF that included both in-plane translations and rotations. The baseline structural properties of the beam elements are $EA = 6.784 \times 10^7$ N (1.525×10^7 lb), $EI = 8.205 \times 10^8$ N-cm^2 (2.859×10^7 lb-in.^{2}), a distributed mass for all members $\bar{m} = 0.846$ kg/cm (1.900×10^{-3} lb-s^2/in.^{2}), and two large concentrated masses of magnitude, $M = 8307.8$ kg. Only 32 in-plane translational DOF were assumed instrumented (Fig. 3c), and Guyan reduction was used to reduce the full analytical model from 168 DOF to the initial (undamaged) experimental model having 32 DOF.

A total of five cases were studied, each representing a different damage scenario. These cases are described in Table 1, and refer to damaged members shown in Fig. 3. In all cases, $S_{\epsilon\epsilon}$ was based on 2% standard deviations of the modal frequencies and the maximum modal displacements of each mode retained in the assessment. Members suspected of damage were weighted equally with S_{RR} based on 15% standard deviations of the baseline material's Young modulus.

Structure A

The natural frequencies of vibration for the first six modes of structure A are given in Table 2. The baseline frequencies f_0 are identical to the finite element method (FEM) frequencies f_a since both were produced from the same analytical model. Thus no MAC or orthogonality checks were required. The frequencies associated with the damaged structure f_d and their shift from the baseline frequency f_0 for all five cases are given in Table 2. The amount of frequency shift is considered extremely small. For example, in case 1 there is no frequency shift for mode 2, whereas in case 2 there is no frequency shift for the first mode. In addition, the frequencies of case 2 are generally larger than those of case 1 as a result of the 5% mass reductions of M. As more members are damaged without loss of mass (cases 3 and 4), there is a slight increase in the frequency shift of modes 2–6, as a result of reductions in f_d. It is interesting to note that the additional damages associated with cases 3 and 4 do not alter the frequency of the first mode.

The residual forces for mode 1 are shown in Fig. 4 for all four cases. The forces were calculated using Eq. (6b), where K_a and M_a are the finite element matrices. The residual forces acting at the nodes for which no value is given in Fig. 4 were 3–4 orders of magnitude smaller than those shown. The residual forces for case 1 give a clear indication that member 6 is damaged since the residual forces are equal and opposite and act at the ends of member 6 (i.e., force balance). For case 2, the residual forces again give an indication that member 6 is damaged and that there exists a change at DOF 13 and 14 that can be associated with either a potential loss of mass or instrumentation error (no force balance). The residual forces for case 3 indicate that members 6 and 7 may be damaged from a nodal force balance. Likewise, the residual forces for case 4 give an indication that members 6, 7, and 24 may be damaged. The forces for mode 1 appear to also indicate the

Table 1 Case studies for assessment

Case	Structure	Comments
1	A	10% stiffness loss in member, Ω_6
2	A	10% stiffness loss in member, Ω_6, 5% loss of M
3	A	Two members with stiffness loss, $\Omega_6 = 10\%$, $\Omega_7 = 5\%$
4	A	Three members with stiffness loss, $\Omega_6 = 10\%$, $\Omega_7 = 5\%$, $\Omega_{24} = 5\%$
5	B	10% stiffness loss in one member, Ω_{11}

Table 2 Case studies for assessment, structure A

	Natural frequency, Hz									
			Case 1		Case 2		Case 3		Case 4	
Mode	f_0	f_a	f_d	$f_0 - f_d$	f_d	$f_0 - f_d$	f_d	$f_0 - f_d$	f_d	$f_0 - f_d$
1	0.499	0.499	0.496	0.003	0.499	0.0	0.496	0.003	0.496	0.003
2	2.212	2.212	2.212	0.000	2.222	−0.010	2.211	0.001	2.204	0.008
3	3.144	3.144	3.126	0.018	3.157	−0.013	3.125	0.019	3.125	0.019
4	7.109	7.109	7.105	0.004	7.157	−0.048	7.101	0.008	7.078	0.031
5	9.815	9.815	9.814	0.001	9.932	−0.117	9.814	0.001	9.808	0.007
6	11.646	11.646	11.638	0.008	11.649	−0.003	11.635	0.011	11.630	0.016

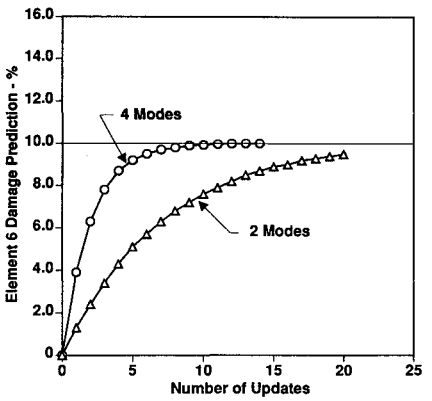

Fig. 5 Structure A damage assessment results, case 1.

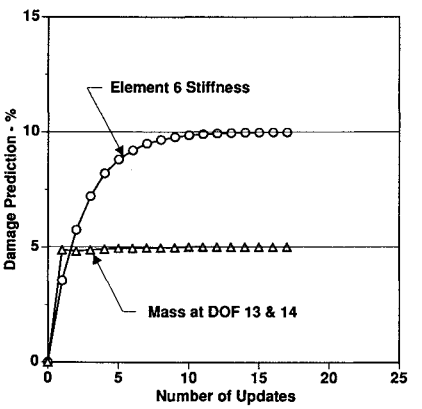

Fig. 7 Structure A damage assessment results using four modes, case 3.

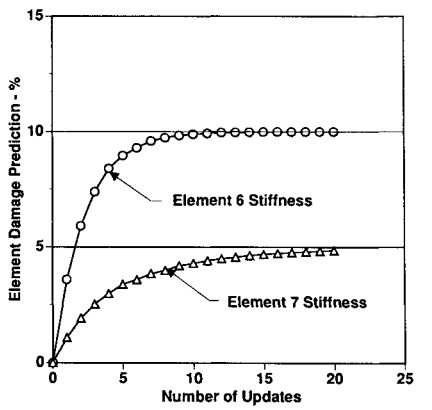

Fig. 6 Structure A damage assessment results using four modes, case 2.

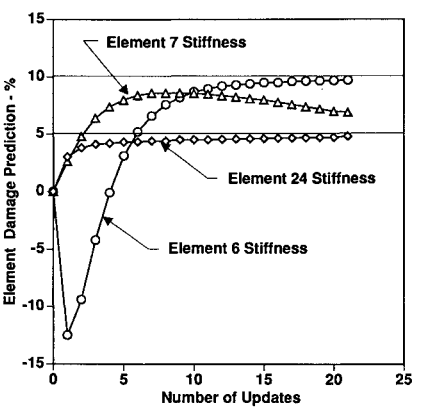

Fig. 8 Structure A damage assessment results using six modes, case 4.

relative extent of damage among the members. This is generally not true if damaged members are located near a node line, since the modal displacements and thus the residual forces will be small.

The results of the assessment of damage severity are shown in Figs. 5–8, where the predicted damage in terms of percent of baseline value is plotted as a function of number of updates. All results show convergence to the exact result and give a precise indication of the severity of member damage. The effect of retaining a larger number of modes in the assessment is to increase the rate of convergence, as evident in case 1 (Fig. 5), which compares the results using the first two modes with that using the first four modes. Cases 2 and 3 (Figs. 6 and 7) both used the first four modes, and case 4 (Fig. 8) used the first six modes. For all cases, S_{RR} was used in lieu of S^*_{RR} in Eq. (10a) and therefore remained constant. It was found that using S^*_{RR} in Eq. (10a) as defined by Eq. (10b) resulted in a slightly slower rate of convergence.

Structure B

The natural frequencies for the first four modes of structure B are given in Table 3. The major frequency shift occurs in mode 3, where the difference in the baseline f_0 and postflight (damaged) frequencies f_d is 0.009 Hz. The accuracy of the Guyan reduced FEM used as the analytical model in the assessment is shown to be very good in the first three modes. However, the FEM's frequency of $f_a = 7.921$ Hz. for the fourth mode shows a significant discrepancy ($f_0 - f_a$) compared to the frequency shift due to damage ($f_0 - f_d$). Modes higher than the fourth mode were found to have an even greater discrepancy between f_0 and f_a. The values for the MACs are also given in Table 3. Good correlation exists between the mode shapes of the first four modes of the baseline and analytical FEM, as well as the baseline and postflight

Table 3 Natural frequencies and modal assurance criteria, structure B

	Natural frequency, Hz					MAC	
Mode	f_0	f_a	f_d	$f_0 - f_a$	$f_0 - f_d$	ϕ_0, ϕ_a	ϕ_0, ϕ_d
1	0.554	0.555	0.552	−0.001	0.002	0.999	0.999
2	2.704	2.706	2.704	−0.002	0.000	0.999	0.999
3	3.313	3.315	3.304	−0.002	0.009	0.999	0.998
4	7.827	7.921	7.826	−0.094	0.001	0.997	0.996

modal test data. The cross-orthogonality check between the FEM and measured baseline data is summarized in Table 4. It is apparent that the fourth mode of the baseline data is not sufficiently orthogonal to the FEM modes, as reflected in the value of 0.795 on the diagonal and 0.028 on the off diagonal. Thus, it is therefore advisable to include only the first three modes in the assessment of damage.

The calculated residual forces of mode 1 are shown in Fig. 9. Calculated residual forces at nodes not shown are 3-4 orders of magnitude smaller than those shown. The residual forces indicate that damage has occurred in either one or both of the elements between the residual forces (elements 11 and 12). It was determined that damage had occurred only in element 11 by noting that the residual forces of Fig. 9 diminish when assigning a nonzero variance only to this member and proceeding with one update in the damage severity assessment. When assigning nonzero variances to both elements 11 and 12, the residual forces increased after performing one update. The assessment for damage severity thus preceded with a nonzero variance assigned only to element 11.

The results of the severity of damage assessment are shown in Fig. 10. The curve labeled Guyan I corresponds to using the first three modes, Guyan II the first four modes, and Guyan III the hypothetical situation of a perfectly correlated FEM with respect to the first four modes (e.g., $\Lambda_a = \Lambda_0$). The results for Guyan I converge to a result of 11%, whereas Guyan II converges to 34%, and Guyan III converges to the exact result of 10%. It is apparent that the use of an incorrect fourth mode (comparing Guyan II with Guyan I) is causing the method to overpredict the severity of damage in member 11 by correcting for discrepancies between Λ_a and Λ_0, whereas, if the exact fourth mode were known (comparing Guyan III with Guyan I), then the method would produce the exact results. As noted earlier, mode 4 was determined to be incorrect (based on cross-orthogonality checks) and should not be used in the assessment, indicating the importance of performing and examining the results of the modal correlation analysis before performing the damage assessment for severity. In the event that one does not have a sufficient number of correlated modes, one could use the current damage assessment algorithm (or existing system identification methods[12-15]) to first correct the analytical model. This is accomplished by using λ_0 and ϕ_0 in Eq. (6b) to locate areas in the FEM needing adjustment and using the vibration characteristics for Λ_0 and Λ_a,

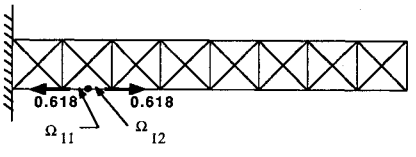

Fig. 9 Mode 1 residual forces for structure B, case 5.

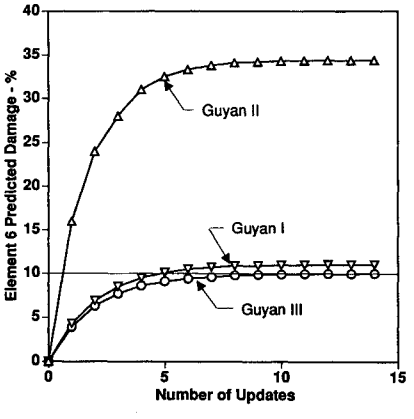

Fig. 10 Structure B damage assessment results, case 5.

Table 4 Cross-orthogonality check, structure B

		FEM ϕ_a			
	Mode	1	2	3	4
Test ϕ_0	1	0.999	0.001	0.001	0.011
	2	−0.004	0.999	0.003	0.008
	3	0.003	0.006	0.990	0.009
	4	0.013	0.028	0.015	0.795

instead of Λ_0 and Λ_d, in Eq. (10a) to determine the necessary correction for the FEM.

As a final comment, the differences in f_0 and f_d are small as well as those of f_0 and f_a and, in the practical sense, less than the resolution of most modal testing equipment. It would be expected in a real application involving modal testing that the differences between f_0 and f_d would be greater as well as those between f_0 and f_a. The results of this study are still considered valid since it is the relative differences between $(f_0 - f_d)$ and $(f_0 - f_a)$ that are important.

Conclusions

A methodology has been presented for detecting structural damage in elastic structures. Measured modal data along with a correlated analytical structural model are used first to locate potentially damaged regions using residual modal force vectors and then conduct a weighted sensitivity analysis to assess the extent of mass and/or stiffness variations, where damage is characterized as a stiffness reduction. The current approach is unique among all existing approaches in that it accounts for 1) variations in system mass, system stiffness, and mass center locations; 2) perturbations of both the natural frequencies and modal vectors; and 3) statistical confidence factors for the structural parameters and potential experimental instrumentation error. Numerical results using a two-dimensional space truss structure clearly illustrate the following:

1) It is important to have a "baseline" analytical model that is correlated with an initial (undamaged) structural configuration via an experimental modal survey. The modal set of the baseline model must pass a modal assurance criteria (MAC) and a cross-orthogonality check (COR) before it can be deemed acceptable. The current approach can be used as a system identification method to correlate the analytical model with an initial (undamaged) modal survey.

2) The residual force approach can locate regions within a structure that are associated with potential damage, mass changes, and/or instrumentation errors. This approach works exceptionally well even if the frequency shift is negligible.

3) The magnitude of damage or mass variations can be accurately determined using the weighted sensitivity analysis, where the rate of convergence depends on the number and quality of the modal vectors.

4) The method works exceptionally well using either a full or reduced analytical model, where the reduced model involved using Guyan reduction to reduce out all translational and rotational DOF not associated with an instrumentation location.

Acknowledgments

The study was supported in part through the first author's participation in the NASA/American Society for Engineering Education Summer Faculty Research Fellowship Program at the NASA Johnson Space Center (JSC), directed by Stanley Goldstein. The authors wish to extend their appreciation to David Hamilton of NASA/JSC for his interest and encouragement, Tim Cao of NASA/JSC for the fruitful discussions on system identification and for providing member sizes and material properties for typical space-type structures, and to Robert Coleman of Lockheed Corporation for the valuable discussions concerning modal correlation techniques and providing typical confidence factors for the instrumentation.

References

[1]Ewins, D. J., *Modal Testing: Theory and Practice,* Wiley, New York, 1984, pp. 233–236.

[2]Vandiver, J. K., "Detection of Structural Failure on Fixed Platforms by Measurement of Dynamic Response," *Proceedings of the Offshore Technology Conference,* Vol. 2, Society of Petroleum Engineers, Richardson, TX, 1975, pp. 243–252; also Paper OTC-2267.

[3]Coppolino, R. N., and Rubin, S., "Detectability of Structural Failures in Offshore Platforms by Ambient Vibration Monitoring," *Proceedings of the Offshore Technology Conference,* Vol. 1, Society of Petroleum Engineers, Richardson, TX, 1980, pp. 101–110; also Paper OTC-3865.

[4]Cawley, P., and Adams, R. D., "A Vibration Technique for Non-Destructive Testing of Fibre Composite Structures," *Journal of Composite Materials,* Vol. 13, No. 3, 1979, pp. 161–175.

[5]Adams, R. D., Crawley, P., Pye, C. J., and Stone, B. J., "A Vibration Technique for Non-Destructively Assessing the Integrity of Structures," *Journal of Mechanical Engineering Science,* Vol. 20, No. 2, 1978, pp. 93–100.

[6]Crawley, P., and Adams, R. D., "The Location of Defects in Structures from Measurements of Natural Frequencies," *Journal of Strain Analysis,* Vol. 14, No. 1, April 1979, pp. 49–57.

[7]Park, Y. S., Park, H. S., and Lee, S. S., "Weighted-Error-Matrix Application to Detect Stiffness Damage by Dynamic Characteristic Measurement," *Journal of Modal Analysis,* Vol. 6, No. 2, 1988, pp. 101–107.

[8]Stubbs, N., and Osegueda, R., "Global Non-Destructive Damage Evaluation in Solids," *International Journal of Analytical and Experimental Modal Analysis,* Vol. 5, No. 2, 1990, pp. 67–79.

[9]Smith, S. W., and Hendricks, S. L., "Evaluation of Two Identification Methods for Damage Detection in Large Space Trusses," *Proceedings of the 6th VPI&SU/AIAA Symposium on Dynamics and Controls for Large Space Structures,* Virginia Polytechnic Inst. and State Univ., Blacksburg, VA, 1987, pp. 127–142.

[10]Chen, J.C., and Garba, J.A., "On-Orbit Damage Assessment for Large Space Structures," *AIAA Journal,* Vol. 26, No. 12, 1988, pp. 1119–1126.

[11]Stubbs, N., Broome, T. H., and Osegueda, R., "Nondestructive Construction Error Detection in Large Space Structures," *AIAA Journal,* Vol. 28, No. 1, 1990, pp. 146–152.

[12]White, C. W., and Maytum, B. D., "Eigensolution Sensitivity to Parametric Model Perturbations," *Shock and Vibration Bulletin,* Vol. 46, No. 5, 1976, pp. 123–133.

[13]Kabe, A. K., " Stiffness Matrix Adjustment Using Mode Data," *AIAA Journal,* Vol. 23, No. 9, 1985, pp. 1431–1436.

[14]Chen, T. Y., and Wang, B. P., "Finite Element Model Refinement Using Modal Analysis Data," *Proceedings of the AIAA/ASME/ASCE/AHS 29th Structures, Structural Dynamics, and Materials Conference,* Vol. II, AIAA, Washington, DC, 1988, pp. 1219–1229.

[15]Collins, J. D., Hart, G. C., Hasselman, T. K., and Kennedy, B., "Statistical Identification of Structures," *AIAA Journal,* Vol. 12, No. 2, 1974, pp. 185–190.

[16]Fox, R. L., and Kapoor, M. P., "Rates of Change of Eigenvalues and Eigenvectors," *AIAA Journal,* Vol. 6, No. 12, 1968, pp. 2426–2429.

[17]Nelson, R. B., "Simplified Calculation of Eigenvector Derivatives," *AIAA Journal,* Vol. 14, No. 9, 1976, pp. 1201–1205.

[18]Mills-Curan, W. C., "Calculation of Eigenvector Derivatives for Structures with Repeated Roots," *AIAA Journal,* Vol. 26, No. 7, 1988, pp. 867–871.